scientific reports

Check for updates

OPEN

Analysis of thermal wave scattering and temperature distribution in sub-surface, defects of gradient construction materials

Xujiao Yang[1], Jinlei Gai[2]✉, Xinliang Zheng[1]✉, Yi Xie[1]✉, Xiaomiao Yu[2], Ruizhi Gong[1], Zhongqing Meng[1], Shuo Zhai[1] & Xunlong Zhao[1]

Traditional building materials have significant limitations in function and performance: insulation materials are easy to peel and age, waterproof materials have a short life, and fireproof materials have degraded flame retardancy. These shortcomings cannot meet the needs of modern buildings for energy efficiency, safety and durability. Therefore, it is imperative to study gradient building materials that integrate function and structure. In this study, based on the non-Fourier heat conduction law, a heat wave propagation model is established to derive a complete analytical solution for the heat wave scattering field of a subsurface circular defect in an exponentially gradient material. The effects of thermal diffusion length (μ/a), wave number (ka), non-uniformity coefficient ($\sigma_1 a$), and defect embedding ratio (b/a) on the surface temperature distribution are systematically analysed by the wavefunction expansion method and the virtual mirror technique combined with the independently developed numerical procedure. The results show that: the peak temperature amplitude occurs in the region directly in front of the scatterer; the thermal fluctuation effect is significantly enhanced with the increase of the thermal diffusion length or the decrease of the defect size; the temperature fluctuation response is strengthened by the high modulation frequency (large ka) and the shallow burial depth of the defects; and the increase of the non-uniformity parameter of the material $\sigma_1 a$ results in the increase of the surface temperature. The study confirms the limitations of traditional Fourier's law in short-pulse heat conduction scenarios, and the results provide theoretical basis and data support for the design of functional gradient materials and nondestructive inspection by infrared thermography.

Keywords Gradient Building materials, Non-Fourier law, Thermal wave scattering, Temperature distribution, Subsurface defects

Gradient building materials, also known as functionally graded materials (FGMs), refer to new composite materials with continuous changes in composition and structure along the thickness or length direction, resulting in gradient changes in performance. FGMs are composed of two or more materials, with different performance materials at both sides and gradient changes in the middle material, properties, and functions, fully leveraging the advantages of both materials. FGMs feature gradient variations in physical parameters, including thermal conductivity, specific heat, and density[1]. FGMs have diverse applications in engineering. They serve as thermal protection coatings, spacecraft re-entry shields, and optical gradient refractive index materials. These versatile materials unlock innovative solutions in various fields. Gradient materials are now extensively utilized across multiple domains: tissue engineering[2,3]materials science[4–6]optics[7,8]biomedical science[9,10]aerospace engineering[11]and automation technologies[12].

Currently, most building materials use traditional basic building materials such as concrete, steel, wood, brick, and block. Traditional building materials have many shortcomings. For example, The original insulation material is layered glue, causing material peeling and strength reduction over time, unable to meet the efficient insulation needs. Traditional waterproof materials are simply coated and pasted, causing material aging and tensile strength reduction over time, unable to meet efficient waterproof needs. Traditional fireproof materials are stacked layer by layer, causing material shedding over time, exposing the material and reducing flame retardant performance, unable to meet efficient fireproof needs. Therefore, studying gradient materials integrating

[1]School of Civil Engineering and Transportation, Beihua University, Jilin 132013, China. [2]Forestry College, Beihua University, Jilin 132013, China. ✉email: 2944708745@qq.com; g2944708745@163.com; 18104323306@163.com

functionality and structure is considered. Gradient building materials demonstrate superior performance and efficiency compared to traditional building materials in terms of function and performance. FGM has the following advantages: (1) Through carefully designed composition structure and physical parameter adjustment, FGM can effectively enhance the bonding strength between different material interfaces; (2) Differentiation of functions or properties within the same material is achieved, thus achieving excellent interface bonding effect; (3) In complex and variable usage environments, FGMs can also maintain the stability and matching of its performance, ensuring that the material will not be damaged. This makes the applicability of FGMs greater than traditional building materials, suitable for pursuing higher performance, safer, and multifunctional building material fields. Traditional basic materials are often combined with new types of insulation, heat insulation, waterproof, fireproof, and other functional materials to form a multifunctional, multi-gradient complex structural system meeting the higher requirements of modern buildings for energy efficiency, safety, and function. Gradient building materials can better adapt to external environmental changes. For example, in cold regions, the bottom uses high thermal resistance materials to maintain temperature and reduce heat loss, while the top uses high reflective materials to reduce solar radiation absorption and decrease heat energy, achieving energy-saving and emission reduction effects. By enhancing fibers, particles, and strengtheners through gradient distribution, the overall strength, seismic performance, and comprehensive performance of the material can be improved while reducing structural weight. FGMs can avoid temperature changes and reduce thermal stress. For example, in building construction, different parts of the house have different temperature requirements, necessitating the use of FGMs with varying thermal conductivity rates for material design. This allows effective control of heat conduction in different parts of the house and reduces thermal stress impact and damage on building construction.

There are numerous methods for fabricating FGMs, including but not limited to 3D printing, powder metallurgy, vapor deposition, and electrodeposition. However, during the fabrication process, FGMs inevitably develop micro-defects, which can impact their overall performance[13]. Among the advanced modern fabrication techniques, 3D printing undoubtedly leads in the field of FGMs preparation. This technology achieves a gradual transition of material properties from one surface to another by precisely controlling the layer-by-layer deposition of multiple materials, successfully fabricating FGMs. Notably, cracks can be observed in the linearly graded structures of FGMs manufactured through laser-based 3D printing[14]. Additionally, 3D concrete printing technology has brought innovation to the construction industry, providing both lightweight and robust functionally graded building materials[15]. With 3D printing, it becomes feasible to construct walls using high-performance insulating materials, which can reduce energy demands in both residential and commercial settings[16]. Remarkable achievements have also been made in small-scale construction projects[17]. Many scholars both domestically and internationally have conducted in-depth research on 3D printing technology for FGMs. For instance, Valizadeh[18] and his team employed grayscale digital processing within FGMs 3D printing technology to successfully develop materials with specific hyperelastic properties and realize functionally graded structures with limited deformation. These studies provide valuable experience and guidance for 3D printing technology in FGMs.

Recent advancements in non-Fourier heat conduction theory have further expanded the understanding of thermal wave behaviors in heterogeneous materials. The Guyer-Krumhansl equation, which incorporates both temporal and spatial relaxation effects, has been widely applied to study thermal wave propagation in FGMs. For instance, Yadav et al.[19–22] investigated wave propagation in porous micropolar fractional-order thermoelastic diffusive media under initial stress using generalized thermoelasticity theory, exploring the modulation of quasi-plane waves (qLD/qT/qMD/qTD) in rotating orthotropic magneto-thermoelastic diffusive media via Lord-Shulman theory. Further studies analyzed reflection characteristics and energy distribution of coupled plane waves in rotating magneto-thermoelastic half-spaces with impedance boundaries, as well as wave reflection in nonlocal porous-thermo-micropolar diffusive half-spaces based on memory-dependent derivative (MDD) thermoelasticity. Meanwhile, in optoelectronic FGMs, Lotfy et al.[23–26] uncovered the magneto-thermo-electro-elastic coupling in elastic semiconductors under hydrostatic stress and mechanical loads via dual-phase-lag photothermal theory. Their work further revealed 2D magneto-elastic-plasma-thermal transport in rotating semiconductors with microtemperature fields, and 1D elastic-plasma-thermal wave coupling induced by Hall currents in semiconductor rods under strong magnetic fields. Complementarily, Alharbi et al.[27] proposed exact solutions (trigonometric, hyperbolic, rational) for photothermal transport equations using exp(-f(ζ))-expansion and finite difference methods, validating solution stability. Ismail et al.[28] demonstrated temperature-dependent thermo-electro-elastic wave interference in microstretch semiconductors via variable thermal conductivity models.

Computer simulation analysis is an effective method for designing FGMs. L.J. Gray studied the classical Fourier heat conduction of exponential gradient materials. Nevertheless, in scenarios involving laser pulse heating, the conventional Fourier heat conduction theory encounters constraints. Wave theory signifies progress beyond the conventional Fourier law of heat conduction by incorporating relaxation properties of thermal energy transfer. If the heat carrier's wavelength aligns with the structural feature's length scale, or if the heat transfer period is less than the time needed for thermal equilibrium, wave-like characteristics will be observed in the heat transfer process. Since the 1990s, researchers worldwide have extensively studied the challenges of thermal conduction resulting from short pulse laser heating and the complex scattering of thermal waves in homogeneous materials with subsurface defects. Reza V H[29] and colleagues employed a radial point interpolation technique to investigate wave propagation in FGMs subjected to thermal conditions, demonstrating its greater convenience and accuracy compared to the moving least squares method. Daneshjou[30] and colleagues conducted research grounded in the principles of non-Fourier heat conduction, employing an advanced state-space methodology to investigate heat transfer within a two-dimensional functionally graded material (FGMs) hollow cylinder subjected to a transient heat source. Their findings revealed that an elevation in the thermal conductivity

ratio results in a reduction of non-Fourier temperature distribution along the radial axis. In a separate study, Jiang[31] and team utilized a non-Fourier heat conduction model, incorporating complex function theory and mapping techniques, to examine thermal wave scattering in the vicinity of apertures within platinum-rhodium fiberglass leak plate structures, offering a thorough examination of the phenomenon. Najibi[32] and his research group undertook an examination of the axisymmetric heat conduction equation in two dimensions, focusing on hollow cylindrical structures fabricated from one-dimensional FGMs, through the application of hierarchical finite element methods. Yaghoobi[33] and colleagues applied first-order temperature theory and energy methods to study the performance of inner and outer layers in cylindrical bodies of varying thicknesses and the impact of heterogeneity on cooling and heating curves. AK Kheibari[34] and colleagues employed the Cattaneo-Vernotte theory to delve into deriving an analytical solution for non-axisymmetric temperature profiles within large-scale multilayer composite cylinders. Their research revealed that material inhomogeneities exert a substantial influence on both the temperature distribution and thermal deformation of functionally graded cylinders. Salari[35] and his team conducted research on the nonlinear dynamic snap-through buckling and vibrational behavior of thermally post-buckled functionally graded (FG) porous nanobeams, focusing on their response under static and sudden mechanical loads, grounded in the theory of nonlocal elasticity.In a separate study, Zeighami[36] adopted the complex variable approach to investigate thermal stresses in porous plates composed of asymmetric functionally graded carbon nanotube-reinforced composites (FG-CNTRC) under conditions of uniform heat flux. Likewise, Najibi A et al.[32] utilized the finite difference approach to explore heat conduction in FGMs at steady-state, grounding their analysis in classical theories. Han[37] along with his team, conducted an analysis of the steady-state and transient heat transfer processes in FGMs by utilizing a coupled thermomechanical model within the finite element software MultiFracS. He[38] along with his team, conducted an extensive study on the influences of the distribution characteristics of elastic modulus, the properties of thermal expansion coefficient, and the features of fracture toughness of FGMs on the material, specifically focusing on the processes of thermal damage, crack formation, and crack propagation. Kushnir[39]in collaboration with his team, devised an innovative polynomial approach for the investigation of thermoelastic wave propagation within functionally graded material plates, grounded on the principles of the Green-Nagdhi thermoelastic theory. Collectively, these investigations build upon classical thermal diffusion principles while advancing the analytical framework through specialized computational techniques, thereby establishing a robust foundation for modeling thermal wave scattering in functionally graded materials.

The presence of defects in materials can lead to numerous scattering events of thermal waves, causing changes in the amplitude and phase of the surface temperature. Measuring these changes using a laser thermal wave detection system can obtain internal structural information of materials for detection and flaw detection purposes. Thermal wave nondestructive testing technology can not only timely detect tiny defects in materials and prevent potential safety hazards but also provide valuable experimental basis for the optimization design of materials, promoting the continuous progress and development of aerospace technology, and has important significance in the research of new materials for aerospace, among other issues.

This section studies the scattering of circular holes on thermal waves and surface temperature distribution in exponential gradient materials based on heat transfer theory. A comprehensive solution for the scattering field has been successfully formulated through the application of the wave function expansion method in conjunction with the virtual image technique, and an associated numerical computation program has been devised.

Heat fluctuation equation and answer

The structure under investigation is a semi-infinite one, characterized by its FGMs composition. A spherical column, which serves as a thermal insulator, has a radius of 'a' and is located at a depth of 'b' below the surface. A modulated ultrashort laser pulse with frequency f is directed along the z-axis, causing the material surface to heat up and initiating a thermal wave process within the solid, as illustrated in Fig. 1.

The gradient building materials studied in this paper adopt an exponential component distribution characteristic, with their core physical parameters (thermal conductivity λ and specific heat capacity c_p) exhibiting an exponential variation along the material thickness direction. Specifically, this is expressed as: $\lambda = \lambda_0 \exp(2\sigma z)$, $c_p = c_{p_0} \exp(2\sigma z)$, where z is the material depth coordinate; λ_0 and c_{p_0} are the reference values at the surface; and σ is the non-uniformity parameter. This exponential grading design achieves a smooth transition of thermal properties by continuously adjusting the material's internal microstructure. Compared to traditional segmented

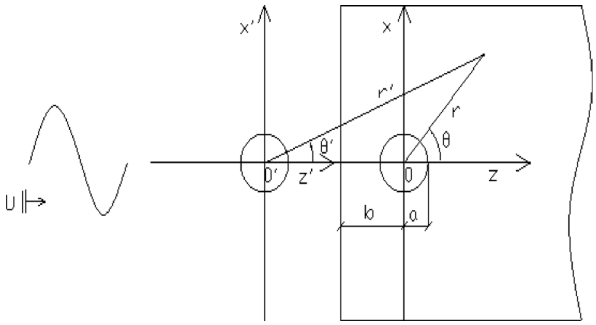

Fig. 1. Modulated light wave incident on semi-infinite FGMs.

grading materials, it offers superior interface bonding strength and thermal shock resistance. The mathematical simplicity of the exponential model makes it particularly suitable for analytical modelling, effectively describing the propagation and attenuation characteristics of heat waves in non-uniform media.

Among them, *a* is the radius of the adiabatic spherical column, *b* is the burial depth, and *f* is the frequency.

The equation describing temperature distribution in gradient materials, derived from the non-classical Fourier law of heat conduction, is presented below:

$$\nabla \cdot (\lambda \nabla T) = \rho c_p \left(\frac{\partial T}{\partial t} + \tau \frac{\partial^2 T}{\partial t^2} \right) \tag{1}$$

where T is the temperature inside the gradient material; The Hamilton operator is represented by ∇, $\nabla = \frac{i\partial}{\partial x} + \frac{j\partial}{\partial y} + \frac{k\partial}{\partial z}$; The symbols λ is the thermal conductivity, c_p is specific heat at constant pressure, and ρ is density of FGMs, respectively; τ denotes the thermal relaxation time. Assuming constant density and thermal relaxation time, the thermal conductivity and specific heat at constant pressure exhibit an exponential trend:

$$\lambda = \lambda_0 \exp(2\sigma z) \tag{2a}$$

$$c_p = c_{p0} \exp(2\sigma z) \tag{2b}$$

In this formula, λ_0 and c_{p0} denote the complex thermal conductivity and the specific heat at constant pressure when $z=0$; σ denote the spatial variation indices for the material's thermal conductivity and specific heat, reflecting the material's non-uniformity parameters that can be represented as complex variables, specifically $\sigma = \sigma_1 + i\sigma_2$.

By substituting Eq. (2) into Eq. (1), the resulting equation is acquired:

$$\nabla^2 T + 2\sigma \frac{\partial T}{\partial z} = \frac{1}{c^2} \frac{\partial^2 T}{\partial t^2} + \frac{1}{D} \frac{\partial T}{\partial t} \tag{3}$$

D represents the thermal diffusivity, which is a constant; $D = \frac{\lambda}{\rho c_p} = \frac{\lambda_0}{\rho c_{p0}}$ is a constant; The speed of thermal wave propagation is represented by c, $c = \sqrt{\frac{D}{\tau}}$.

The steady-state periodic solutions of the problem under investigation will be examined and analyzed. We define the complex amplitude function $\vartheta(x,y,z)$ such that the total temperature field is expressed as: $T = T_0 + Re\left[\vartheta\, exp\left(-i\omega\, t\right)\right]$. T is the ambient temperature; *Re* denotes the real part of a complex quantity; $\vartheta(x,y,z)$ represents the spatially dependent complex amplitude of the temperature fluctuation; ω is the angular frequency of thermal wave excitation. After separating variables by $T = T_0 + Re\left[\vartheta\, exp\left(-i\omega\, t\right)\right]$, the temperature control Eq. (3) can be reduced to the following form:

$$\nabla^2 \vartheta + 2\sigma \frac{\partial \vartheta}{\partial z} + \left(\frac{\omega^2}{c^2} + \frac{i\omega}{D} \right) \vartheta = 0 \tag{4}$$

T_0 denotes average temperature of the environment; ω denotes angular frequency, $\omega = 2\pi f$; The imaginary unit is $i = \sqrt{-1}$.

The particular solution to Eq. (4) is given and displayed in the mathematical form below:

$$\vartheta = \exp(-\sigma z) u(x, y, z) \tag{5}$$

The $u(x,y,z)$ satisfies the given equation:

$$\nabla^2 u + \kappa^2 u = 0 \tag{6}$$

The complex wave number k is a key parameter for thermal waves, $k = \left(\frac{\omega^2}{c^2} + \frac{i\omega}{D} - \sigma^2 \right)^{1/2} = \alpha + i\beta$, comprising two parts: α and β. α the wave number associated with thermal wave propagation. while β represents absorption coefficient of thermal waves.

$$\alpha = \sqrt{\frac{1}{2} \left\{ \sqrt{\left[\kappa^2 - \sigma^2\right]^2 + \frac{\omega^2}{D^2}} + \left[\kappa^2 - \sigma^2\right] \right\}} = \sqrt{\sqrt{\frac{1}{4}\left[\kappa^2 - \sigma^2\right]^2 + \frac{1}{\mu^4}} + \frac{1}{2}\left[\kappa^2 - \sigma^2\right]} \tag{7}$$

$$\beta = \sqrt{\frac{1}{2} \left\{ \sqrt{\left[\kappa^2 - \sigma^2\right]^2 + \frac{\omega^2}{D^2}} - \left[\kappa^2 - \sigma^2\right] \right\}} = \sqrt{\sqrt{\frac{1}{4}\left[\kappa^2 - \sigma^2\right]^2 + \frac{1}{\mu^4}} - \frac{1}{2}\left[\kappa^2 - \sigma^2\right]} \tag{8}$$

In the absence of diffusion effect (undamped), $k = \frac{\omega}{c}$, $\mu = \sqrt{\frac{D}{\omega}}$. μ the thermal diffusion length, D is the thermal diffusivity, c is the propagation speed of thermal waves. When $c \to \infty$,the expressions for α and β simplify:

$$\alpha \to \sqrt{\sqrt{\frac{1}{4}\sigma^2 + \frac{1}{\mu^4}} - \frac{1}{2}\sigma^2} \tag{9a}$$

$$\beta \to \sqrt{\sqrt{\frac{1}{4}\sigma^2 + \frac{1}{\mu^4}} + \frac{1}{2}\sigma^2} \tag{9b}$$

After analysis, it is recognized that a fluctuation process in the form of $\vartheta\, e^{-i\omega\, t} = \vartheta_{\,0} e^{-(\beta + \sigma_{\,1})x} e^{i[(\alpha - \sigma_{\,2})x - \omega\, t]}$ occurs in FGMs, representing a propagating temperature wave with decaying vibration amplitude in the z direction.

The Eq. (4) determines the general solution for the thermal wave scattering field within FGMs, providing an exhaustive and precise account:

$$\vartheta = \exp(-\sigma x) \sum_{n=0}^{\infty} \sum_{m=-\infty}^{\infty} A_{mn} h_n^{(1)}(\kappa r) P_n^m(\cos\theta) e^{im\phi} \tag{10}$$

This general solution is derived via separation of variables in spherical coordinates. The expression for the first-order spherical Hankel function, denoted as $h_n^{(1)}(\cdot)$, is provided in the form of $h_n^{(1)}(x) = \sqrt{\pi / 2x}\, H^{(1)}_{n+1/2}(x)$. The Hankel function of the second kind is denoted by $H_n^{(1)}(\cdot)$, the associated Legendre function is represented by $P_n^m(\cdot)$, and the scattering wave mode coefficient A_{mn}, which originates from subsurface defects, is determined by the boundary conditions related to those defects.

Thermal wave excitation, incidence, and overall wave field characteristics

Modulated ultrashort pulse laser beams can generate heat waves on the surface of gradient materials, resulting in a steady-state thermal wave that propagates along the positive z-axis on the material's surface. The incident wave, in accordance with Bloch wave propagation theory, can be described as follows:[40].

$$\vartheta_1^{(i)} = \vartheta_0 \exp(i\kappa b) \exp(-\sigma z) \exp\left[i\left(\kappa z - \omega t\right)\right] \tag{11}$$

ϑ_0 is temperature amplitude of thermal waves; k is the wave number of the incident waves; $j_n(\cdot)$is the spherical Bessel function; $P_n(\cdot)$ is the Legendre polynomial.

The scattered waves generated by the virtual images characterize the reflected waves at the boundary of a semi-infinite body. The formula for the mirror incident waves propagating in the negative direction along the z' axis is provided as follows:

$$\vartheta_2^{(i)} = \vartheta_0 \exp(i\kappa b) \exp(-\sigma z') \exp\left[-i\left(\kappa z' + \omega t\right)\right] \tag{12}$$

In (r,θ,ϕ) the thermal wave scattering field generated by subsurface defects is a complex phenomenon, with its expression given as follows:

$$\vartheta_1^{(s)} = \exp\left[-\sigma r \cos\theta\right] \sum_{n=0}^{\infty} A_n^l h_n^{(1)}(\kappa r) P_n(\cos\theta) \exp(-i\omega t) \tag{13}$$

In the mirrored local coordinate system, which is defined by the coordinates (r',θ',ϕ') representing the radial, polar, and azimuthal directions respectively, the scattered waves that emerge from subsurface defects can be fully described and characterized:

$$\vartheta_2^{(s)} = \exp\left[\sigma r' \cos\theta\right] \sum_{n=0}^{\infty} B_n^l h_n^{(1)}(\kappa r') P_n(\cos\theta') \exp(-i\omega t) \tag{14}$$

The thermal wave mode coefficients of scattering are denoted as A_n^l and B_n^l ($l = 1,2,\ldots\ldots,\infty$), determined by satisfying boundary conditions. The adiabatic boundary condition at the defect surface ($r = a$, where a is the defect radius) requires:

$$\frac{\partial \vartheta}{\partial n}\Big|_{r=a} = -\frac{\partial \vartheta}{\partial r}\,|_{r=a} = 0 \tag{15}$$

When describing the boundary characteristics of a defective cylinder, the variable n is used to represent the normal direction of the boundary.

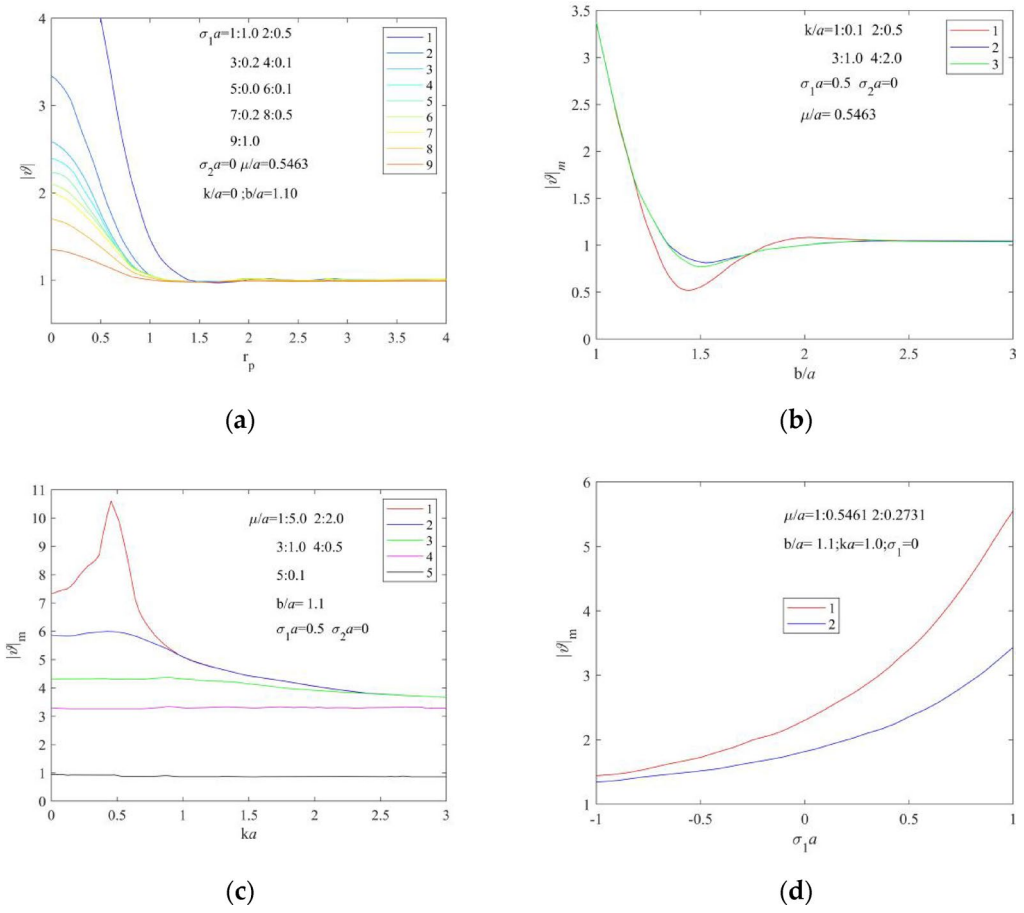

Fig. 2. This is a figure. Schemes follow another format. If there are multiple panels, they should be listed as: (**a**) Temperature distribution on the surface of the object; (**b**) The effect of burial depth on the maximum surface temperature; (**c**) The impact of wave number on the maximum surface temperature; (**d**) The influence of inhomogeneous parameter burial depth on the maximum surface temperature.

Ignoring the time factor, the surface temperature distribution of FGMs has this mathematical expression:

$$\vartheta = \vartheta_0 \exp(\mathrm{i}\kappa \mathrm{b}) \exp(-\sigma \mathrm{z}) \exp(\mathrm{i}\kappa \mathrm{z}) + \exp(-\sigma \mathrm{z}) \sum_{l=1}^{\infty} \sum_{n=1}^{\infty} A_n^1 h_n^{(1)}(\kappa r) P_n(\cos\theta) + \exp(-\sigma \mathrm{z}') \sum_{l=1}^{\infty} \sum_{n=1}^{\infty} (-1)^n A_n^1 h_n^{(1)}(\kappa r') P_n(\cos\theta') \tag{16}$$

This research investigation concentrates on adiabatic boundary conditions associated with subsurface defects, where the characteristic length is designated as the radius a of the subsurface spherical cylinder. The amplitude of the incident temperature is denoted by the given value $|\vartheta_0|$. Utilizing the non-dimensional parameter defined below: non-diffusive traveling wave number, denoted as ka, with a range of $ka = 0.01 \sim 3.0$. The relative thermal diffusion length, denoted as μ/a, falls within the range of $\mu/a = 0.1 \sim 5.0$. The real part of the inhomogeneity parameter is $(\sigma_1 a) = 0.01 \sim 1.0$, the imaginary part is $(\sigma_2 a) = 0.01 \sim 1.0$. The burial ratio is $b/a = 1.1 \sim 3.0$; temperature ratio ϑ/ϑ_0. And, the complex wave number in dimensionless form is given by ka, with $ka = \alpha a + i\beta a$.

Numerical example

The wave number $ka = 0$ and the inhomogeneous parameter $\sigma = 0$ in Fig. 2(a) correspond to the pure thermal diffusion case without fluctuation terms in the heat equation for a homogeneous material. As can be seen from Fig. 2(a), the results of the temperature analysis calculations on the surface of the gradient material are consistent with the theory. At this time, the parameters are: the heat diffusion coefficient $D = 75\mathrm{mm}^2/\mathrm{s}$, the radius of the hole is $a = 2.0$ mm, and the buried depth is $b = 2.2$ mm. curve 1 and curve 2 correspond to the temperature distribution when the frequency is $f = 20$ Hz,$f = 80$ Hz respectively. And it can be seen that the larger the relative thermal diffusion length, the larger the temperature change. The maximum value of the temperature is obtained at the right-angle coordinate (0,0,-b).

It can be seen from Fig. 2(b) that the effect on the temperature starts when the relative thermal diffusion length is small and the wave number *ka* is relatively large, e.g. $ka = 1.0$. i.e., when the thermal diffusion length is small or the defect size is large, the effect of the fluctuation in the heat transfer is negligible. The change in temperature amplitude decreases when the defects are buried at larger depths. Again, it can be seen that the effect of volatility in heat propagation is weak when the wave number *ka* is small.

As can be seen in Fig. 2(c), the effect of volatility on temperature in heat transfer is greater when the thermal diffusion length is larger or the defect size is smaller. When the wave number *ka* is relatively large, it corresponds to high-frequency vibration (short-wave case), when the corresponding heat propagation characteristics have a particle nature.

As can be seen in Fig. 2(d), when the thermal diffusion length is large, the surface temperature of the gradient material increases as the non-uniform coefficient $\sigma_1 a$ increases.

Conclusion

This paper offers a comprehensive approach to addressing the scattering of thermal waves in exponential gradient materials via the thermal conduction wave model. The research involved meticulous and systematic calculations to examine the variation trends of the temperature amplitude across diverse parameters, and the corresponding alterations in the temperature amplitude were represented by plots on relevant curves. These curves visually demonstrate the propagation of thermal waves and their impact on temperature in exponential gradient materials under various factors.

1) Particularly in the area directly in front of the scatterer, it is observed that the amplitude of temperature variation attains its highest value.
2) Larger thermal diffusion length or smaller defect size increases the wave-like behavior effect on temperature.
3) Higher modulation frequency of the incident temperature increases the wave-like behavior effect on temperature.
4) Shallower defect burial depth intensifies the defect's impact on temperature.

In certain conditions, the traditional Fourier's law of heat conduction fails to accurately describe thermal wave propagation, requiring consideration of wave effects. Focusing on the impact of subsurface defects on heat conduction highlights the importance of wave effects. The presence of defects can notably influence the propagation and energy distribution of thermal waves, resulting in substantial effects on the material as a whole. The research outcomes offer a theoretical basis and reference data, contributing to the investigation of functionally gradient materials and the interpretation of infrared thermal imaging.

Data availability

The datasets used and/or analysed during the current study available from the corresponding author on reasonable request.

Received: 17 March 2025; Accepted: 6 June 2025
Published online: 01 July 2025

References

1. Zhang, R. et al. Review of additive manufacturing techniques for large-scale metal functionally graded materials[J]. *Crystals* **12** (6), 858 (2022).
2. Bonfanti, A., Domenicale, L. & Bhaskar, A. 3D printing of functionally graded films by controlling process Parameters[J]. *Comput. Aided Tissue Eng.: Methods Protoc.* **2147**, 31–42 (2021).
3. Abdel-Gawad, D. R. I. et al. Therapeutic effect of mesenchymal stem cells on histopathological, immunohistochemical, and molecular analysis in second-grade burn model[J]. *Stem Cell Res. Ther.* **12**(1), 308 (2021).
4. Kong, X. et al. Manufacturing and characterization of functionally gradient material from cemented carbide to diamond via filament-based material extrusion 3D printing[J]. *Additive Manuf.* **91**, 104325 (2024).
5. Boggarapu, V. et al. State of the Art in functionally graded materials[J]. *Compos. Struct.* **262**, 113596 (2021).
6. Yevtushenko, A., Topczewska, K. & Zamojski, P. Influence of thermal sensitivity of functionally graded materials on temperature during braking[J]. *Materials* **15** (3), 963 (2022).
7. Chen, B. et al. *Development and Characterization of 316L/Inconel625 Functionally Graded Material Fabricated by Laser Direct Metal deposition[J]*123105916 (Optics & Laser Technology, 2020).
8. Mehrabi, O., Seyedkashi, S. M. H. & Moradi, M. *Experimental and Response Surface Study on Additive Manufacturing of Functionally Graded steel-inconel Wall Using Direct Laser Metal deposition[J]*167109707 (Optics & Laser Technology, 2023).
9. Pragya, A. & Ghosh, T. K. Soft functionally gradient materials and Structures–Natural and manmade: A Review[J]. *Adv. Mater.* **35** (49), 2300912 (2023).
10. Saleh, B. et al. 30 years of functionally graded materials: an overview of manufacturing methods, applications and future Challenges[J]. *Compos. Part. B: Eng.* **201**, 108376 (2020).
11. Zhao, H. et al. Finite element analysis for residual stress of TC4/Inconel718 functionally gradient materials produced by laser additive manufacturing[J]. *Opt. Laser Technol.* **152**, 108146 (2022).
12. Halim, Q. et al. Metallic glass properties, processing method and development perspective: a review[J]. *Int. J. Adv. Manuf. Technol.* **112**, 1231–1258 (2021).
13. Li, Y., Wang, T. & Zhou, M. Impact response characteristics and meso-evolution mechanism of functionally gradient brittle materials with pore hole damage[J]. *Compos. Struct.* **256**, 112989 (2021).
14. Shang, C. et al. Eliminating the crack of laser 3D printed functionally graded material from TA15 to Inconel718 by base preheating[J]. *Opt. Laser Technol.* **126**, 106100 (2020).
15. Tay, Y. W. D. et al. Creating functionally graded concrete materials with varying 3D printing parameters[J]. *Virtual Phys. Prototyp.* **17** (3), 662–681 (2022).
16. Góra, M., Bańkosz, M. & Tyliszczak, B. Use of innovative methods to produce highly insulating walls using 3D-printing technology[J]. *Materials* **17** (16), 3990 (2024).

17. Akman, A. & Sadhu, A. Recent development of 3D-Printing technology in construction Engineering[J]. *Pract. Periodical Struct. Des. Constr.* **29** (1), 03123005 (2024).
18. Valizadeh, I. et al. Tailoring of functionally graded hyperelastic materials via grayscale mask stereolithography 3D printing[J]. *Additive Manuf.* **47**, 102108 (2021).
19. Yadav, A. K. Thermoelastic waves in a fractional-order initially stressed micropolar diffusive porous medium[J]. *J. Ocean. Eng. Sci.* **6** (4), 376–388 (2021).
20. Yadav, A. K. Magnetothermoelastic waves in a rotating orthotropic medium with diffusion[J]. *J. Eng. Phys. Thermophys.* **94** (6), 1628–1637 (2021).
21. Yadav, A. K. Effect of impedance on the reflection of plane waves in a rotating magneto-thermoelastic solid half-space with diffusion[J]. *AIP Adv.*, **10**(7), 075217 (2020).
22. Yadav, A. K. et al. Effects of memory response and impedance barrier on reflection of plane waves in a nonlocal micropolar porous thermo-diffusive medium[J]. *Mech. Adv. Mater. Struct.* **31**(22), 5564–5580 (2024).
23. Lotfy, K., Elidy, E. S. & Tantawi, R. S. Photothermal excitation process during hyperbolic two-temperature theory for magneto-thermo-elastic semiconducting medium[J]. *Silicon* **13** (7), 2275–2288 (2021).
24. Lotfy, K., El-Bary, A. A. & El-Sharif, A. H. Ramp-type heating microtemperature for a rotator semiconducting material during photo-excited processes with magnetic field[J]. *Results Phys.* **19**, 103338 (2020).
25. Lotfy, K. et al. Hall current influence of microtemperature magneto-elastic semiconductor material[J]. *Superlattices Microstruct.* **139**, 106428 (2020).
26. Lotfy, K. & El-Bary, A. A. Magneto-photo-thermo-microstretch semiconductor elastic medium due to photothermal transport process[J]. *Silicon* **14** (9), 4809–4821 (2022).
27. Alharbi, A. R., Almatrafi, M. B. & Lotfy, K. Constructions of solitary travelling wave solutions for Ito integro-differential equation arising in plasma physics[J]. *Results Phys.* **19**, 103533 (2020).
28. Ismail, G. M. et al. Influence of variable thermal conductivity on thermal-plasma-elastic waves of excited microelongated semiconductor[J]. *Alexandria Eng. J.* **61** (12), 12271–12282 (2022).
29. Reza, V. H., Hui, Z. & ,Wennan, Z. An efficient Meshfree computational approach to the analyze of thermoelastic waves of functionally graded materials in a two-dimensional space[J]. *Alexandria Eng. J.* **61** (12), 10495–10510 (2022).
30. Das, P., Islam, M. & ,Hasib, M. Corrective and new research frontier of dual-phase -lag non-fourier heat conduction in functionally graded cylindrical materials with bi-directional property variations[J]. *Int. J. Thermofluids* **24**, 100861 (2024).
31. Jiang, W. et al. Thermal wave scattering and temperature concentration around the opening in Platinum–Rhodium leaky Plates[J]. *Metals* **10**(7), 946 (2020).
32. Najibi, A. & Wang, H. G. Two-Dimensional C-V Heat conduction investigation of an FG-Finite axisymmetric Hollow Cylinder[J]. *Symmetry* **15**(5), 1009 (2023).
33. Yaghoobi, P. M. & Ghannad, M. An analytical solution for heat conduction of FGM cylinders with varying thickness subjected to non-uniform heat flux using a first-order temperature theory and perturbation technique[J].*Int. Commun. Heat Mass Transf.* **116**, 104684 (2020).
34. Kheibari, K. A., Jafari, M. & Nazari, B. M. Propagation of heat wave in composite cylinder using Cattaneo- Vernotte theory[J]. *Int. J. Heat Mass Transf.* **160**, 120208 (2020).
35. Salari, E. et al. Nonlinear dynamic buckling and vibration of thermally post-buckled temperature-dependent FG porous nanobeams based on the nonlocal theory[J]. *Phys. Scr.* **97** (8), 085216 (2022).
36. Zeighami, V. & Jafari, M. Thermal stress analysis of perforated unsymmetric FG-CNTRC plate using a general analytical solution[J]. *Thin-Walled Struct.* **173**, 108956 (2022).
37. Han, D. et al. Heat conduction and cracking of functionally graded materials using an FDEM-based thermo-mechanical coupling model[J]. *Appl. Sci.* **12** (23), 12279 (2022).
38. He, D., Huang, D. & Jiang, D. *Modeling and Studies of Fracture in Functionally Graded Materials Under Thermal Shock Loading Using peridynamics[J]*111102852 (Theoretical and Applied Fracture Mechanics, 2021).
39. Kushnir, R. M., Zhydyk, U. V. & Flyachok, V. M. Thermoelastic analysis of functionally graded cylindrical shells[J]. *J. Math. Sci.* **254** (1), 46–58 (2021).
40. Hu, C., Fang, X. Q. & Du, S. Y. *Multiple Scattering of Thermal Waves from a Subsurface Spheroid in Exponentially Graded Materials Based on non-Fourier's model[J]*5070–77 (Infrared physics & technology, 2007). 1.

Author contributions

Conceptualization, X.Y., J.G., X.Z. and Y.X.; methodology, X.Y.; software, X.Y.; validation, X.Y., J.G., X.Z. and Y.X.; formal analysis, X.Y.; investigation, X.Z. and Y.X.; resources, X.Y., J.G., X.Z., Y.X., X.Y., Z.M., S.Z., Y.Z., and Z.G.; data management, Z.M.; writing—original draft preparation, X.Y.; writing—review and editing, X.Y.; visualization, J.G. and X.Z.; supervision, Y.X.; project administration, S.Z.; funding acquisition, X.Y. All authors have read and agreed to the published version of the manuscript.

Funding

This research was funded by the Key New Technology Development and Verification Service for the Transformation and Upgrading Project of Jilin Chemical Industry Group (Phase 3), grant number 2024 2202 0200 0363.

Declarations

Competing interests

The authors declare no competing interests.

Disclaimer

The statements, opinions and data contained in all publications are solely those of the individual author(s) and contributor(s) and not of MDPI and/or the editor(s). MDPI and/or the editor(s) disclaim responsibility for any injury to people or property resulting from any ideas, methods, instructions or products referred to in the content.

Additional information

Correspondence and requests for materials should be addressed to J.G., X.Z. or Y.X.